ASSESSEMENT OF POTENTIAL FOR DRAG REDUCTION USING A BOX-WING CONFIGURATION

S. Braun, T. Lammering, K. Risse, R. Hörnschemeyer
Institut für Luft- und Raumfahrt der RWTH Aachen
Wüllnerstraße 7, 52062 Aachen, Deutschland

Abstract

The Box-Wing is a non-planar aircraft conf guration that is composed of two wings joined by winglets. In the scope of this paper aerodynamic eff ciency of this conf guration is investigated. The focus thereby does not lie on the induced drag alone; also viscous as well as wave drag is taken into account. Inf uences of the wing design parameters on the aircraft's aerodynamic eff ciency are investigated. Aerodynamic calculations are conducted with an in-house tool. It includes a multiple lifting-line method combined with an extended f at-plate solution for turbulent f ow. A semi-empirical methodology is applied to determine transonic effects. The tool is applicable to arbitrary aircraft conf gurations.
In order to identify the main design parameters and the inf uences on the aerodynamic eff ciency, a parameter study is conducted. For inviscid drag calculations the aerodynamic eff ciency increases with enlarged vertical offset of both wings. The aerodynamic optimum, however, is shifted towards smaller gaps for viscous f ow. Furthermore, an optimum was determined for two Box-Wing conf gurations with two different applications – short-range and long-range aircraft. These optimized designs are then compared against two aircraft in conventional conf guration.

Nomenclature

η	Dynamic viscosity [$\frac{kg}{m \cdot s}$]
λ	Taper Ratio
ρ	Density [kg/m^3]
φ_{LE}	Leading edge sweep angle [deg]
AR	Aspect Ratio
b	Wing span [m]
c	Chord length [m]
$C_{D,ind}$	Induced drag coeff cient
$C_{D,misc}$	Drag coeff cient of miscellaneous drag
$C_{D,p_{min}}$	Minimum pressure drag
$C_{D,total}$	Total drag coeff cient
$C_{D,visc}$	Viscous drag coeff cient
$C_{D,wave}$	Wave drag coeff cient
C_F	Skin-friction coeff cient
FF	Form Factor
g/MAC	Relative longitudinal wing displacement
h/b	Relative horizontal wing displacement
k_A	Technology factor of the airfoil
L	Lift [N]
M	Flight Mach number
M_{crit}	Critical Mach number
M_{DD}	Drag divergence Mach number
MAC	Mean Aerodynamic Chord [m]
Q	Interference factor
Re	Reynolds number
S_{wet}	Wetted surface [m^2]
t/c	Thickness to chord
v	Airspeed [m/s]

1. INTRODUCTION

The Box-Wing (BW) is a wing conf guration that is composed of two wings connected at the tips with winglets, see FIG 1. According to literature such non-planar wing conf gurations induce less vortex drag than conventional conf gurations [1], [2], [3]. Theoretical results published by Prandtl [4] indicate that vortex drag of a Box-Wing is up to 50% lower than that of conventional wing conf gurations with equal aspect ratio. Using the lifting line theory, Prandtl showed that a Box-Wing with elliptical lift distribution is the conf guration which induced lowest vortex drag of all possible wing conf gurations. Reduction in structural weight as well as improved control stability characteristics are other possible advantages of Box-Wings often cited [5].

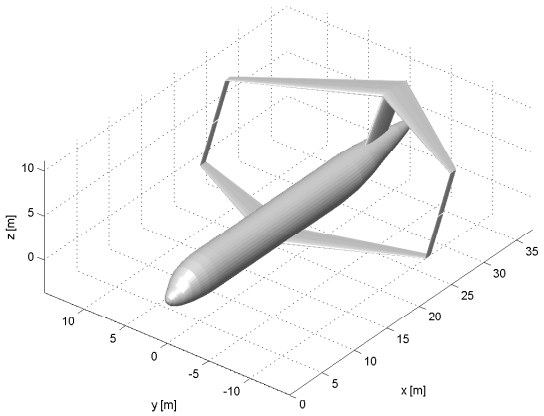

FIG 1. Typical Box-Wing conf guration

The induced drag of today's commercial jet transport aircrafts is typically 40% of total drag in cruise f ight [2]. Hence, halving vortex drag would improve overall aerodynamic eff ciency signif cantly. This makes the Box-Wing a very promising concept for eff cient future transport aircraft.

These assumptions, however, are only valid under inviscid conditions. The goal of this study is to identify the main design parameters of a Box-Wing conf guration also considering viscous and wave drag. Furthermore, a comparison of optimized Box-Wing conf gurations with two baseline tail-aft conf gurations will be performed – short-range and long-range aircraft concepts.

2. PARAMETERS OF BOX-WING GEOMETRY

Typical parameters that inf uence the aerodynamic eff ciency, e.g. aspect ratio (AR) or mean aerodynamic chord (MAC), are def ned differently for Box-Wing conf gurations than for conventional conf gurations. This section brief y introduces the relevant wing parameters that are used throughout this paper.

The mean aerodynamic chord of a Box-Wing can be def ned as the sum of the MAC of the upper and the lower wing [6], Eq. 1. Accordingly, the characteristic Reynolds number (Re) of the complete conf guration is given by Eq. 2. Here, ρ denotes the density of the air, v the airspeed and η the dynamic viscosity of the f uid.

$$MAC = MAC_{upperWing} + MAC_{lowerWing} \tag{1}$$

$$Re = \frac{\rho \cdot v \cdot MAC}{\eta} \tag{2}$$

Another characteristic parameter is the wing reference area (S_{ref}). For a Box-Wing conf guration it is def ned as the sum of the reference areas of the upper and lower wing. Hence, overall aspect ratio is def ned as:

$$AR = \frac{b^2}{S_{ref}} = \frac{b^2}{S_{ref,lowerWing} + S_{ref,upperWing}} \tag{3}$$

The def nition of the wing span (b) remains the same as for conventional tail-aft conf gurations. However, this def nition holds only for conf gurations where span of upper and lower wing is identical.

Since only trapezoid wings will be considered in this paper, the following def nition of taper ratio λ is used:

$$\lambda = \frac{c_{t,lowerWing} + c_{t,upperWing}}{c_{r,lowerWing} + c_{r,upperWing}} \tag{4}$$

The variables c_t and c_r denote the chord length of the wing tip and wing root, respectively.

3. AERODYNAMIC MODELS

The presented studies were conducted with an in-house aero-tool that had been developed by the Institute of Aeronautics and Astronautics (ILR) of RWTH Aachen University. It estimates f ight polars of arbitrary aircraft conf gurations in subsonic and transonic f ight regime. It is fully integrated into the ILR Preliminary Aircraft Design Suite. In the scope of this paper only a brief overview over the underlying methodology is given. A detailed description and comprehensive validation was published by Lammering et al. [7].

3.1. Lift and Induced Drag

The multi-lifting-line tool *LiftingLine* (Release 2.2) is used to estimate lift as well as induced drag within the ILR aero-tool. *LiftingLine* was developed by the German Aerospace Center (DLR) [8], [9]. It allows analyzing of arbitrary non-planar wing conf gurations as shown in FIG 2.

LiftingLine is based on the potential theory. An inviscid, irrotational and steady f ow around slender bodies is modeled by the distribution of a system of singularities and superposition of this system with an undisturbed incoming f ow [10]. Potential theory does not account for non-linear effects. Since the assessment presented in this paper is for cruise condition only, non-linear effects such as f ow separation can be neglected. To account for compressibility, the Prandtl-Glauert correction [11] is applied.

Inf uences of the fuselage as well as engine nacelles on overall induced drag are estimated with semi-empirical correction terms suggested by Roskam [12]. Contribution of these components on total lift are neglected.

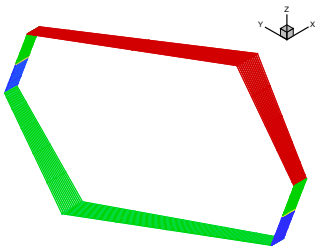

FIG 2. Lifting surface representing a swept Box-Wing

3.2. Viscous Drag

Within the ILR aero-tool viscous drag is estimated by a component built-up method [13]. It is computed based on the skin friction coeff cent (C_F) and a form factor (FF). The skin friction coeff cient is estimated by the f at-plate solution for turbulent f ow [11] using the local Reynolds number Re_{local} of each component, see Eq. 5. The prediction of the form factors varies for each aircraft component [13].

$$C_F = \frac{0.455}{(log_{10}Re_{local})^{2.58} \cdot (1 + 0.144 \cdot M^2)^{0.65}} \quad (5)$$

Additionally, lift dependent viscous drag ($C_{D,visc,lift}$) is estimated by a parabolic correction suggested by Hoerner [14]. It is given by Eq. 6, where $C_{D,p_{min}}$ is the minimum pressure drag coeff cient.

$$C_{D,visc,lift} = C_{D,p_{min}} \cdot C_L^2. \quad (6)$$

Taking interference effects into account, the viscous drag of the overall aircraft conf guration is than estimated by Eq. 7.

$$C_{D,visc} = \frac{\sum C_F \cdot FF \cdot Q \cdot S_{wet}}{S_{ref}} + C_{D,misc} + C_{D,visc,lift}, \quad (7)$$

where S_{wet} is the wetted surface, Q an interference factor, and $C_{D,misc}$ includes further miscellaneous drag components. A detailed description of these parameters can be found in [13].

3.3. Wave Drag

Wave drag is estimated with Lock's approximation as suggested by Malone [15], see Eq. 8. It is determined by the difference between f ight Mach number (M) and critical Mach number (M_{crit}). Wave drag is zero for Mach numbers smaller than the critical one.

$$C_{D,wave} = 20 \cdot (M - M_{crit})^4 \quad (8)$$

According to Malone, the critical Mach number can be estimated with the drag divergence Mach number (M_{DD}), Eq. 9. Finally, M_{DD} is estimated from Korn's equation, which was enhanced to include wing sweep, as shown in Eq. 10, where k_A denotes a technology factor describing the airfoil's transonic characteristics.

$$M_{crit} = M_{DD} - \left[\frac{0.1}{80}\right]^{1/3} \quad (9)$$

$$M_{DD} = \frac{k_A}{cos\varphi_{LE}} - \frac{t/c}{cos^2\varphi_{LE}} - \frac{C_L}{cos^3\varphi_{LE}} \quad (10)$$

Inf uences of the fuselage and other aircraft components on overall wave drag are neglected within the ILR aero-tool.

4. VERIFICATION OF ILR-AERO TOOL TO APPLICATION FOR BOX-WING CONFIGURATIONS

Experimental data from wind tunnel tests of Box-Wing conf gurations are rare. Gall [5] published some data in 1984. He performed tests with a rectangular Box-Wing at Reynolds numbers of 500,000. The wind tunnel model had a semi span of $0.5\ m$ and a chord length of $0.2\ m$. The upper wing was placed one chord length above and one chord length in longitudinal direction behind the lower wing. A symmetric and untwisted wing with a NACA 0012 airfoil was used.

This wind tunnel tests showed large regions of laminar separation at such low Reynolds numbers; total drag increased noticeably. Hence, the minimum drag pressure coeff cient $C_{D,p_{min}}$ (see Eq. 6) cannot be directly applied to determine the viscous drag. Based on wind tunnel tests conducted by Nenadovitch [16], Gall derived a new correlation between lift and drag. This data implies a parabolic correction for lift dependent viscous drag as well. For laminar separation at low Reynolds numbers the drag coeff cient $C_{D,p_{min}}$ is replaced by a constant value of 0.08.

In FIG 3, Gall's wind tunnel test results for lift dependent drag (square symbol) are plotted against calculated induced and lift dependent viscous drag (black curve). A close agreement can be observed. Zero lift drag, however, is not comparable. The wind tunnel tests showed that the boundary layer was partially laminar, whereas the ILR aero-tool estimated friction drag for full turbulent f ow.

Gall also conducted theoretical investigations with a vortex-lattice code. Results of these calculations are also shown (triangle symbol) in FIG 3. This data matches the inviscid drag estimated with *LiftingLine* well (dashed curve).

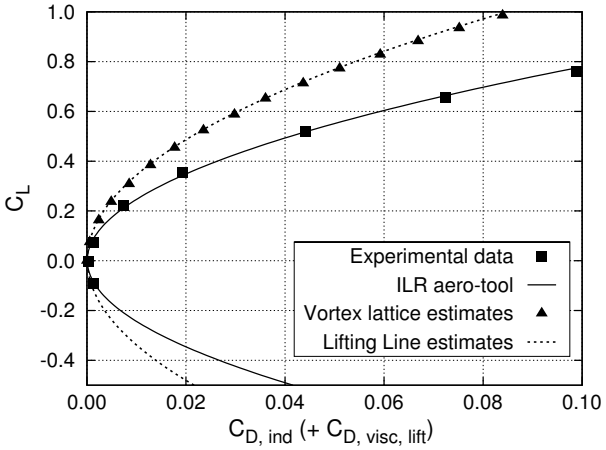

FIG 3. Lift dependent drag

5. PARAMETER STUDY

To identify the inf uence of varying wing geometry and placement of both wings relative to each other on overall drag, a parameter study was conducted. To reduce the number of parameters the reference wing area ratio ($S_{1,ref}/S_{2,ref}$) between the forward and backward wing is

held constant at a value of one in the presented study. The same holds for the angle of incidence of both wings. Furthermore, only untwisted trapezoid wings without kinks were investigated. Integration of engine nacelles was also neglected in the study.

5.1. Reference Area Ratio and Distribution of Lift

Prandtl [4] stated that minimum induced drag is theoretically achieved for equal lift force ratio ($L_1/L_2 = 1$) between both wings. More detailed investigations conducted by Lange et al. [17] show, however, that a non-equal lift force ratio has only minor effect on total induced drag. A penalty in induced drag of only 2% occurs. Thus, to further reduce the number of investigated parameters, changes in angle of incidence were excluded.

5.2. Wing Gap and Angle of Sweep

Wing gap is def ned in vertical as well as in longitudinal direction for Box-Wings. FIG 4 shows the def nition of both parameters. Vertical displacement is generally described by the ratio of the gap in z-direction and span (h/b), whereas longitudinal displacement is described by the ratio of the gap in x-direction and MAC (g/MAC). Longitudinal gap is positive if the upper wing is placed behind the lower wing.

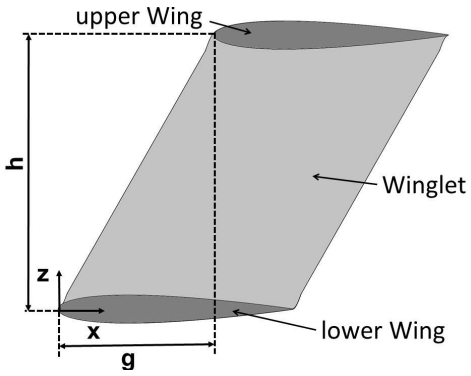

FIG 4. Def nition of Wing gap parameters

According to Prandtl [4], induced drag is reduced by increasing the vertical gap (h/b). He stated that for $h/b = 0.4$ the induced drag is reduced by 45% for example compared to an ideally loaded elliptical monoplane. Munk's theorem [18] states that induced drag is independent of longitudinal staggering if circulation and thus lift is kept unchanged on both wings.

5.2.1 Invicid Calculations

For a rectangular Box-Wing with an aspect ratio of 6 both longitudinal as well as vertical displacement have been varied in this parameter study. In FIG 5 the effects of variation in vertical direction (h/b) on induced drag ratio ($C_{D,ind}/C_{D,ind,ellipt}$) are plotted for different longitudinal offsets (g/MAC). $C_{D,ind,ellipt}$ was calculated for an elliptical monoplane with same aspect ratio from Eq. 11.

$$C_{D,ind,ellipt} = \frac{C_L^2}{\pi \cdot AR} \tag{11}$$

Results in FIG 5 show that the induced drag ratio signif - cantly increases with h/b. The increasing of induced drag ratio shows an asymptotic behavior towards high h/b. For h/b=40% induced drag decreases by 42% compared to the elliptical wing in close agreement with Prandtl [4] whereas a vertical gap of 80% leads towards a drag reduction of 55%. No signif cant changes in induced drag due to horizontal gap can be observed her.

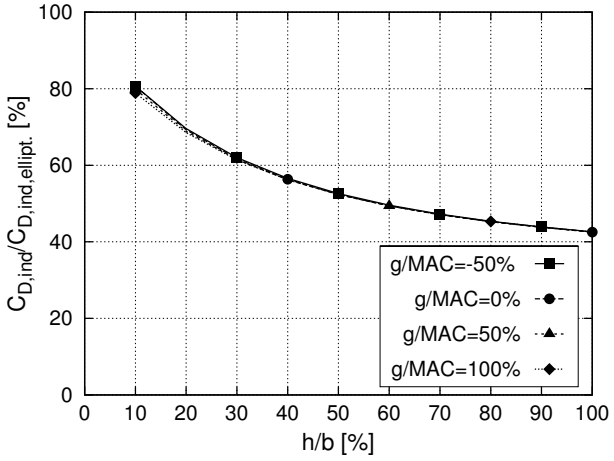

FIG 5. Inf uence of vertical and longitudinal gap on induced drag ratio, $C_L = 0.5$, $AR = 6$

For the rectangular wing, wing root chord as well as wing tip chord are displaced equally, see dashed lines in FIG 6. In a second parameter study the inf uence of the angle of sweep was investigated. The offset of wing root chord varies with sweep angle and span remains constant.

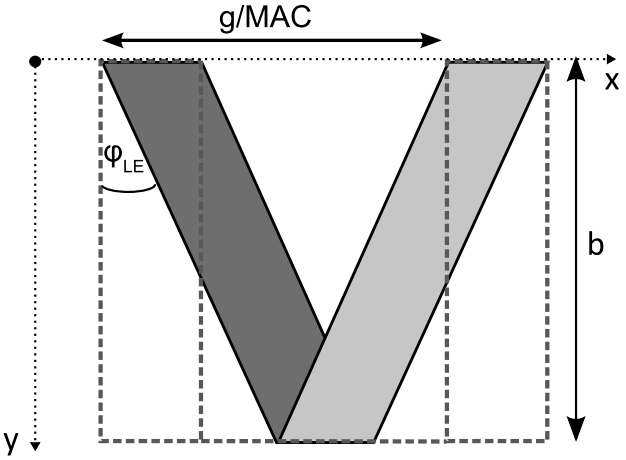

FIG 6. Horizontal offset for rectangular and swept wings

Angle of sweep was varied between 0 and 40 degrees for a wing with an aspect ratio of 6. In FIG 7 effects of variation

in sweep and different longitudinal wing displacements are shown. Minimum induced drag coeff cient is achieved for unswept wings; induced drag eff ciency decreases slightly for increasing sweep. This is caused by changes in the circulation distribution of both wings. Maximum drag penalty, however, is less than 2%. Therefore, the inf uence of longitudinal wing displacement as well as angle of sweep will be neglected in the further studies that are presented here.

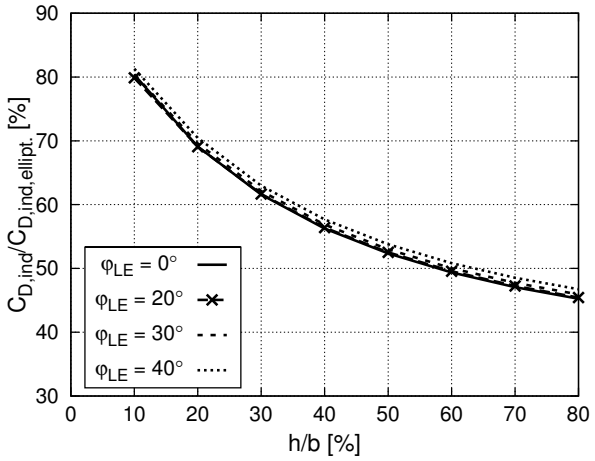

FIG 7. Inf uence of vertical gap and sweep angle on induced drag ratio, $C_L = 0.5$, $AR = 6$

5.2.2 Viscous Calculation

In order to estimate the overall aerodynamic eff ciency of a Box-Wing conf guration, viscous as well as wave drag also have to be considered. Other than for induced drag this includes effects of Reynolds and Mach number. Viscous drag of a Box-Wing is mainly inf uenced by additional wetted surfaces of the winglets when h/b is increased. For realistic Box-Wing conf gurations, the upper wing must be mounted to the fuselage. Therefore, an additional support structure or f n is required for values of h/b exciting the fuselage diameter. Whereas such a structure has no effect on induced drag, viscous drag further increases. Based on today's jet transport aircraft, the authors assumed that maximum fuselage diameter equals a h/b of 0.125.

In FIG 8 the effects of vertical displacements on overall lift-to-drag ratio (L/D) are shown for a constant C_L of 0.5 and varying Mach and Reynolds numbers. Wing sweep was set to 30° and a modern transonic airfoil was used. No fuselage but an additional f n was considered. Compared to FIG 5 the overall optimum in aerodynamic eff ciency shifts towards lower h/b of approximately 15% to 25%, depending on Mach and Reynolds number. As discussed above, additional viscous drag (increased wetted surface) reduces the L/D and thus the eff ciency of the entire conf guration.

With increasing Mach number overall L/D decreases due to wave drag. Neglecting interferences and assuming thin airfoils with large critical Mach numbers as well as small local lift coeff cients, winglets have no effects on wave drag. As the friction coeff cient decreases with Reynolds and Mach number, viscous drag decreases slightly as well. Hence, optimum h/b changes towards higher values.

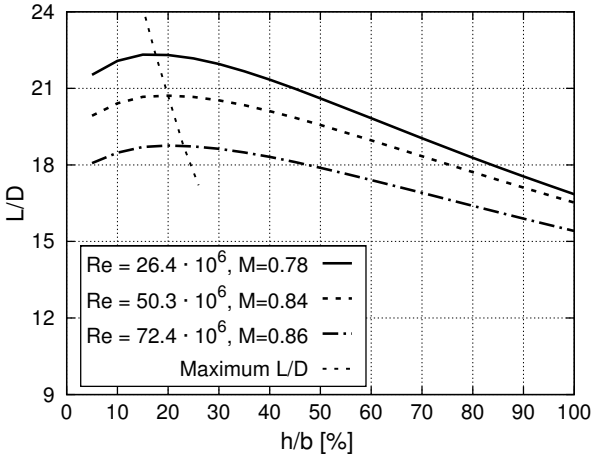

FIG 8. Inf uence of vertical gap on L/D, $C_L = 0.5$, $\varphi = 30°$

5.3. Aspect Ratio

Aspect ratio was identif ed by Khan et al. [19] as one of the primary design parameters for Box-Wings. For conventional aircraft the induced drag coeff cient is reduced by increasing aspect ratio. The same holds for Box-Wings as shown in FIG 9(a). The induced drag coeff cient is plotted against a variation in aspect ratio for different values of h/b. No vertical tail or f n is considered here. The curves show an asymptotic characteristic for induced drag.

In FIG 9(b) the induced drag coeff cients of the Box-Wing is compared to an optimal loaded elliptic wing. Although induced drag can be reduced for all parameter variations, the reduction of induced drag coeff cient is decreased with increasing aspect ratio. Viscous and wave drag are not affected by the aspect ratio as long as Reynolds and Mach number remain constant.

5.4. Taper Ratio

Finally, the inf uences of a variation in taper ratio are discussed. For def nition of taper ratio of Box-Wings see Eq. 4. Reference area and span of both wings are equal as well as the root and the tip chord lengths of both wings. FIG 10(a) implies that the induced drag coeff cient decreases with taper ratio. Minimum induced drag is achieved for a taper ratio of one. Jansen et al. [20] reached the same conclusion when using an optimizer in order to reduce induced drag of arbitrary non-planar wing conf gurations.

In contrast to induced drag, increasing taper ratio leads towards larger viscous drag coeff cients as wetted winglet area increases. For small vertical wing displacements this effect is compensated by a decrease of the induced drag coeff cient. For larger gaps viscous drag penalty predominates, see FIG 10(b). Increasing the value of h/b shifts the optimum taper ratio towards zero. No inf uence of wave drag can be observed as relative wing thickness (t/c) is not affected by taper ratio and, therefore, Eq. 10 is also not affected.

In this chapter only untwisted wings were considered. Further drag reduction could be achieved by modifying the lift distribution. Minimum induced drag would be reached,

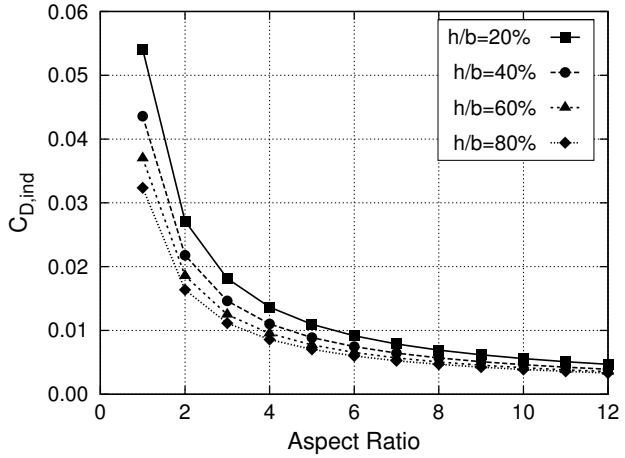

(a) Induced drag

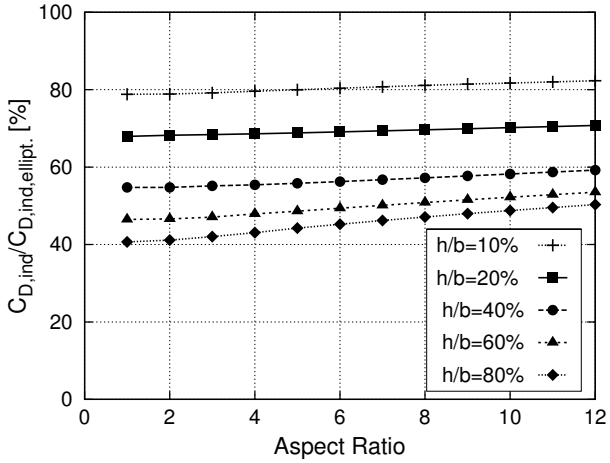

(b) Induced drag ratio

FIG 9. Inf uence of aspect ratio and h/b, $\varphi = 30°$, $C_L = 0.5$

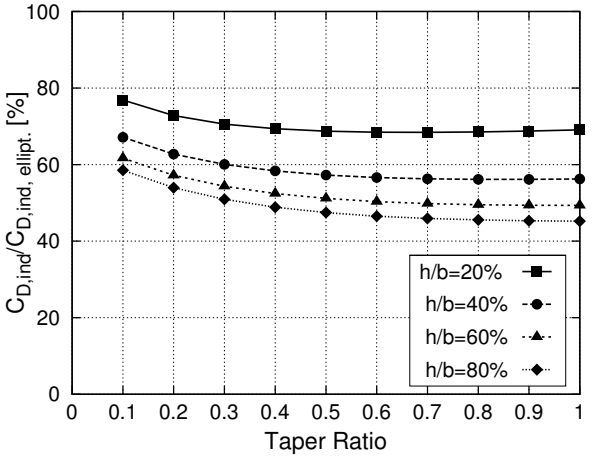

(a) Induced drag ratio

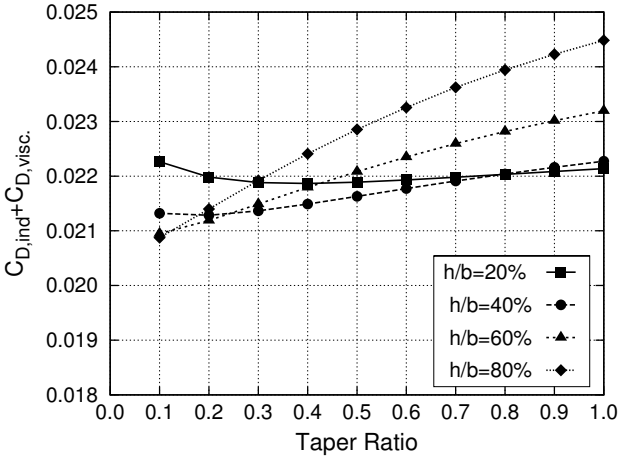

(b) Induced and viscous drag

FIG 10. Inf uence of taper ratio and h/b, $\varphi = 0°$, $C_L = 0.5$, $AR = 6$ and $M = 0.78, Re = 26.4 \cdot 10^6$

when the modif ed lift distribution corresponds to the lift distribution of a so called *'Best-Wing-System'*. Based on the lifting-line theory, Prandtl [4] described such a Box-Wing system which produces minimum induced drag. However, as shown in FIG 11, the potential for further reducing the induced drag coeff cients by an optimized lift distribution is small. Especially untwisted wings with taper ratios bigger than 0.4 seem to provide a lift distribution close to the *'Best-Wing-System'* ones.

As optimum taper ratio also depends on induced drag as well as on viscous drag, an optimization tool will be used in the following chapter to f nd the best taper ratio for the investigated f ight conditions.

6. COMPARISON OF THE BOXWING CONFIGURATION AGAINST STANDARD CONFIGURATION

In order to evaluate the potential of drag reduction on overall aircraft level, Box-Wing conf gurations are compared to two conventional jet transport aircraft in this section.

6.1. Reference Airplanes

As baseline a typical short-range (SR) as well as a long-range (LR) aircraft were chosen. The short-range design is based on an Airbus A320 geometry, the long-range design on a Boeing 777-200, see FIG 12. Integration of engine nacelles was neglected for this study. Typical cruise conditions are M = 0.78 at 30,000 ft for the SR and M = 0.84 at 36,000 ft for the LR. This leads to characteristic Reynolds numbers of 30.6 million (SR), and 47.1 million (LR) respectively.

6.2. Optimization Strategy

In the previous chapter, the vertical wing displacement as well as aspect and taper ratio were identif ed as the most important Box-Wing design parameters. Therefore, these parameters were optimized to derive a Box-Wing conf guration with an optimum wing planform. No wing twist is considered here. The optimization process was conducted using the NOMAD optimization tool [21]. Among others, NOMAD was developed by Boeing Phantom Works to solve complex

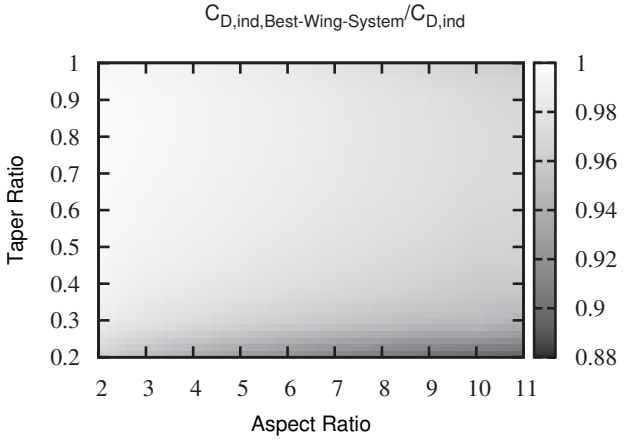

FIG 11. Inf uence of Taper Ratio and Aspect Ratio on Induced drag eff ciency, $C_L = 0.5$, $h/b = 0.25$

A/C	b [m]	S_{ref} $[m^2]$	φ_{LE} [°]	AR	λ	h/b
SR	33.9	125	27.0	9.2	0.24	—
SR-BW	$\leq$ 33.9	125	$\pm$27.0	$\leftrightarrow$	$\leftrightarrow$	$\leftrightarrow$
LR	60.9	451	34.5	8.2	0.29	—
LR-BW	$\leq$ 60.9	451	$\pm$34.5	$\leftrightarrow$	$\leftrightarrow$	$\leftrightarrow$

TAB 1. Aircraft parameters

optimization problems in aircraft design. It uses a mesh adaptive direct search algorithm (MADS) that is backed by an hierarchical non-smooth convergence analysis [22]. NOMAD is fully integrated in the ILR Aircraft Preliminary Design Suite thus enabling optimization of design on an overall aircraft-level.

All other wing parameters were held constant. Furthermore, their values equal the ones of the corresponding reference aircraft. To avoid an excessive increase in span, maximum span for the Box-Wing aircraft was constrained to that of the reference aircraft. A design lift coeff cient of 0.5 is assumed for all aircraft. This leads to equal wing reference area for conventional and Box-Wing aircraft. Tab 1 contains an overview over the different parameters.

The same transonic airfoil was applied to all aircraft. Only exceptions are the winglets of the Box-Wing conf gurations. Thin NACA 0006 airfoils were used here to avoid additional wave drag. Also fuselage remains unchanged for conventional and Box-Wing aircraft. This leads to equal fuselage component drag.

6.3. Optimized Box-Wing

Results of the optimization process are presented in TAB 2. The corresponding Box-Wing conf gurations are plotted in FIG 13. For both conf gurations minimum drag is achieved for maximum allowed span, and for a vertical wing displacement of 13.8% for the short-range conf guration and 14.7%

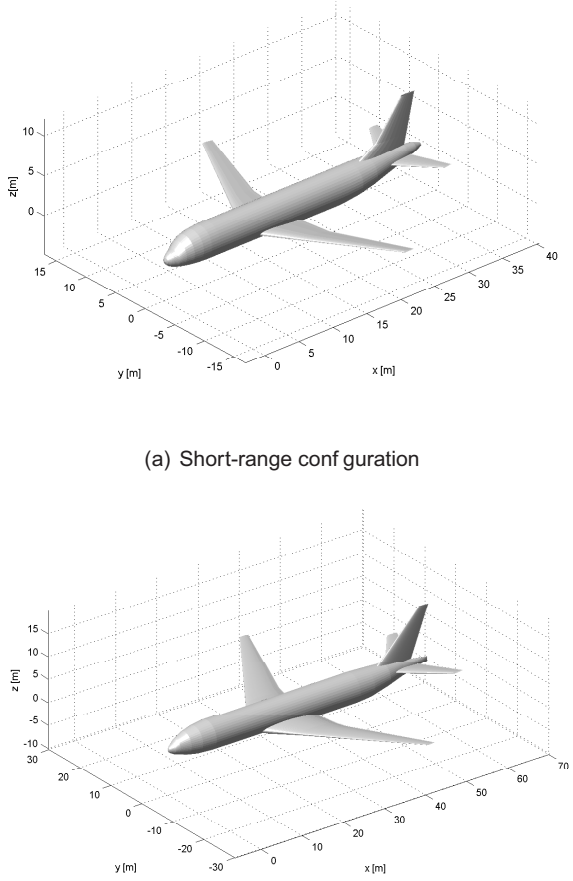

(a) Short-range conf guration

(b) Long-range conf guration

FIG 12. Reference conf gurations

for the long-range. Total drag is reduced by approximately 10% for both aircraft compared against the baseline designs.

A break-down of the drag components of the different conf gurations is shown in FIG 14. Since viscous drag becomes larger for low f ight speeds, the short-range Box-Wing was optimized towards low viscous drag. This was basically achieved by reducing taper ratio. Additionally, the f n and winglet wetted surface is slightly smaller than that of the empennage of the reference aircraft. This leads to the smaller viscous drag of the Box-Wing compared to the baseline short-range conf guration. Induced drag is approximately 17% smaller, while wave drag remains constant. Contrary to the short-range conf guration, the long-range Box-Wing was optimized towards lower induced drag. Whereas viscous drag remains almost constant, induced drag of the Box-Wing is reduced by about 27%. However, stability and control criteria were not checked for the presented designs.

6.4. Trade-off Studies

Since no structural or weight limitations were considered the optimization for aerodynamic eff ciency alone leads to slender wings. Structural weight of such wings can be expected to be quite large thus constraining the wing span

A/C	b [m]	S_{ref} [m^2]	φ_{LE} [deg.]	AR	λ	h/b [%]	$\Delta C_{D,ind}[\%]$	$\Delta C_{D,visc}[\%]$	$\Delta C_{D,total}[\%]$
SR-BW	33.9	125	$\pm$27.0	9.21	0.208	14.7	-17.2	-7.7	-10.7
LR-BW	60.9	451	$\pm$34.5	8.22	0.432	13.8	-27.2	1.4	-9.9

TAB 2. Values for optimized Box-Wing parameters

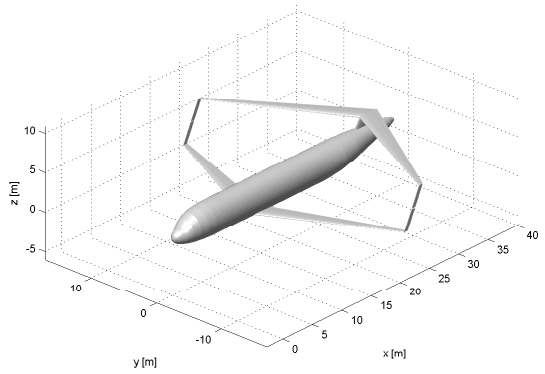

(a) Short-range Box-Wing conf guration (SR-BW)

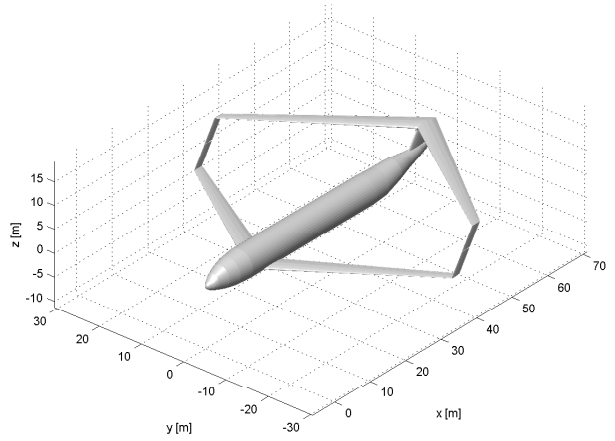

(b) Long-range Box-Wing conf guration (LR-BW)

FIG 13. Optimized Box-Wing conf gurations

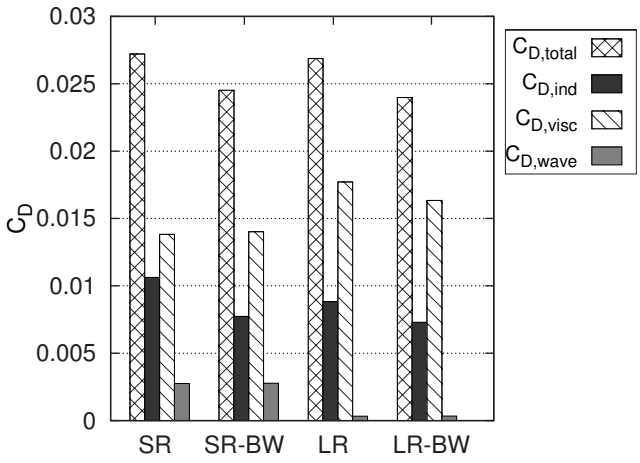

FIG 14. Drag break-down

while keeping reference area constant seems reasonable. A second optimization was conducted to investigate the inf uence of span and aspect ratio accordingly. The constraint in maximum span was f rst reduced by 10% and then by 20%.

A comparison between geometrical parameters of the different Box-Wing conf gurations is shown in TAB 3. Reducing the span by 10% leads towards wings with larger vertical gaps. For the short-range Box-Wing, minimum drag is now achieved at h/b = 20.1% with a taper ratio of $\lambda = 0.22$. Total drag coeff cient for this conf guration is $C_{D,total} = 0.025$. This is equivalent to an overall drag reduction of 6.3% compared to the reference aircraft, see FIG 15(a).

Total drag coeff cient of the new long-range Box-Wing conf guration is approximately 4.8% smaller than total drag of the reference airplane. Here, minimum total drag coeff cient is achieved with a vertical wing gap of 19.2% and a taper ratio of 0.438. For both Box-Wing conf gurations with a span restricted at 80% of the reference airplane, no substantial drag savings could be realized, see FIG 15(b).

6.5. Best-Wing-System

So far, a non optimum lift distribution was examined. Since induced drag of the Box-Wing conf gurations could be further reduced by modifying the wing twist for example, an optimum for induced drag reduction is determined. These calculations are conducted using the results Prandtl obtained for the *'Best-Wing-System'* [4] in place of the invicid *Lifting-Line* calculations. In this case, induced drag only depends on aspect ratio and vertical wing offset. Viscous as well as wave drag are calculated using the ILR aero-tool. In order to minimize the wetted area of the winglets, taper ratio was set to 0.2. The NOMAD-tool was then used to f nd the optimum for aspect ratio and vertical displacement. All other parameters remained unchanged. Results of this optimization are listed in TAB 4. Induced drag of the short-range Box-Wing could be reduced by 32%. This leads towards a total drag reduction of 14.5% compared to the conventional aircraft. For the long-range Box-Wing total drag was reduced by 14.4% compared to the baseline conf guration.

7. CONCLUSION

The goal of this study was to identify the potential for drag reduction using a Box-Wing compared to a conventional tail-aft conf guration. The presented methodology uses a multi-lifting-line method for estimating the induced drag. Viscous drag is estimated with friction coeff cients for turbulent f ow. A semi-empirical method is used for determining wave drag.

A/C	b [m]	S_{ref} [m^2]	φ_{LE} [deg.]	AR	λ	h/b [%]	$\Delta C_{D,ind}[\%]$	$\Delta C_{D,visc}[\%]$	$\Delta C_{D,total}[\%]$
SR-BW	30.5	125	$\pm$27.0	7.76	0.222	20.1	-5.8	-6.6	-6.3
SR-BW	27.1	125	$\pm$27.0	5.90	0.247	28.1	15.9	-5.3	-0.5
LR-BW	54.8	451	$\pm$34.5	6.66	0.438	19.2	-16.3	3.0	-4.8
LR-BW	48.7	451	$\pm$34.5	5.26	0.452	25.2	-1.6	4.6	1.2

TAB 3. Values for optimized Box-Wing parameters with span restrictions

A/C	b [m]	S_{ref} [m^2]	φ_{LE} [deg.]	AR	λ	h/b [%]	$\Delta C_{D,ind}[\%]$	$\Delta C_{D,visc}[\%]$	$\Delta C_{D,total}[\%]$
SR-BW	33.9	125	$\pm$27.0	9.21	0.200	19.2	-32.0	-5.8	-14.5
LR-BW	60.9	451	$\pm$34.5	8.22	0.200	23.1	-40.4	2.3	-14.4

TAB 4. Results for Best-Wing-System

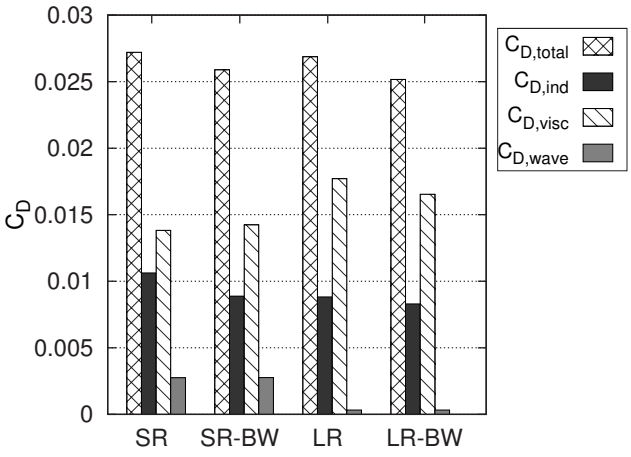

(a) Span limitation: 90% reference span

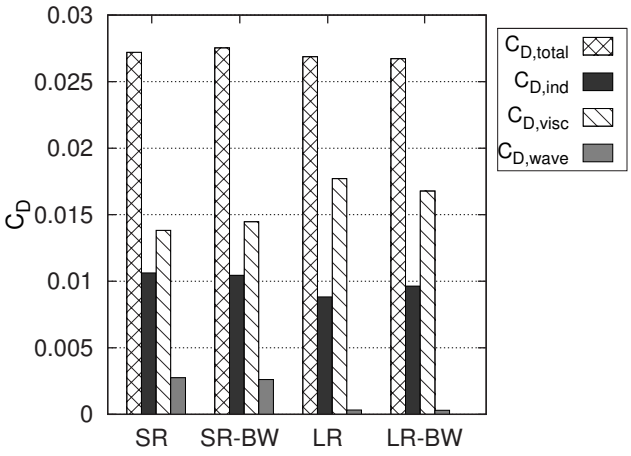

(b) Span limitation: 80% reference span

FIG 15. Drag break-down of Conf guration with span limitations

The presented methodology is applicable to arbitrary conf gurations such as non-planar wings. Main inf uencing factors of Box-Wing drag were identif ed by conducting a parameter study. Vertical wing offset as well as aspect ratio have the strongest inf uence on aerodynamic eff ciency of the Box-Wing conf gurations. Longitudinal offset and wing sweep have negligible inf uence on induced drag. Increasing the taper ratio of the wing reduces induced drag but also increases viscous drag. Therefore, an optimum taper ratio can only be found by considering total drag.

An optimization algorithm was used in order to design two Box-Wing conf gurations for different application – short-range and long-range aircraft. These conf gurations were compared to two baseline tail-aft aircraft (A320 and 777-200). This comparison showed that the overall aerodynamic eff ciency of Box-Wings is higher than that of the conventional conf guration. Total drag could be reduced by approximately 10% for the Box-Wings.

In order to demonstrate the effects of span limitations, a second study was conducted. It was shown that reducing the span by 20% eliminates the aerodynamic advantage of the Box-Wing. Finally, an optimum Box-Wing was examined. In this case total drag of the Box-Wing was reduced by further 4%. This leads towards an overall aerodynamic eff ciency gain of almost 15% compared to the reference aircraft. However, it has to be kept in mind that this is for an ideal scenario.

In a more realistic case additional drag components like wave interference drag near the wing-winglet-joints has to be considered too. Frediani et al. [23] as well as Khan et al. [19] observed strong shock waves in this regions. Probably, such interference effects will further reduce the overall performance of a Box-Wing conf guration.

Aerodynamic eff ciency is not the only variable to be optimized in wing design; wing mass is of equal importance. In further studies an overall optimum towards maximum take-off weight and total fuel eff ciency (block fuel) for an entire aircraft conf guration shall be found. This also includes integration of propulsions as well as stability and control considerations on preliminary design level.

Acknowledgment

The authors would like to thank all colleagues and student assistants of the Institute of Aeronautics and Astronautics that participated in the presented research work.

REFERENCES

[1] J.E. Yates and C. duP. Donaldson, A Fundamental Study of Drag and Assessment of Conventional Drag-Due-to-Lift Reductions Devices, NASA CR-4004, 1986.

[2] I. Kroo, Nonplanar Wing Concepts for Increased Aircraft Eff ciency, VKI lecture series on Innovative Conf gurations and Advanced Concepts for Future Civil Aircraft, 2005

[3] A. Frediani, E. Rizzo, C. Bottoni, J. Scanu, G. Iezzi, A 250 Passenger PrandtlPlane Transport Aircraft Preliminary Design, Aerotecnica Missili e Spazio Vol. 84 4/2005.

[4] L. Prandtl, Induced Drag of Multiplanes, NACA TN 182, 1924

[5] P. D. Gall, An Experimental and Theoretical Analysis of the Aerodynamic Characteristics of a Biplane-Winglet Conf guration, NASA TM 85815, 1984

[6] W. P. Henderson and J. K. Huffman, Aerodynamic Characteristics of a Tandem Wing Conf guration at a Mach Number of 0.30, NASA TM X-72779, 1975

[7] T. Lammering, E. Anton, und R. Henke, Validation of a Method for Fast Estimation of Transonic Aircraft Polars and its Application in Preliminary Design, in Applied Aerodynamics: Capabilities and Future Requirements, 2010

[8] K. Horstmann, Ein Mehrfach-Traglinienverfahren und seine Verwendung fuer Entwurf und Nachrechnung nichtplanarer Flügelanordnungen, DFVLR Forschungsbericht, German Aerospace Center (DLR), 1987.

[9] K. H. Horstmann, T. Engelbrecht, and C. Liersch, A multiple lifting line procedure for design and analysis of nonplanar wings, 2007.

[10] C. M. Liersch and T. F. Wunderlich, A fast aerodynamic tool for preliminary aircraft design, 2008.

[11] E. Truckenbrodt, *Fluidmechanik*, 4th ed. Springer Verlag, 1996, vol. 2.

[12] J. Roskam, *Airplane Design, Part VI: Preliminary Calculation of Aerodynamic, Thrust and Power Characteristics*, 2nd ed. Ottawa, Kansas: Roskam Aviation and Engineering Corporation, 1985, vol. 6.

[13] D. P. Raymer, *Airplane Design: A Conceptional Approach*, 2nd ed. AIAA Education Series, 1992.

[14] S. F. Hoerner, *Fluid-Dynamic Drag*, 1965.

[15] B. Malone and W. H. Mason, "Multidisciplinary optimization in aircraft design using analytic technology models," *Journal of Aircraft*, vol. 32, no. 2, p. 431–438, Apr. 1995.

[16] Nenadovitch and Miroslave, Recherches Sur Les Cellules Biplanes Rigides D'Envergure Inf ne, Publications Scientif gues of Technigue du Ministre de L'Air, 1936

[17] R.H. Lange, J. F. Cahill, E.S. Bradley, R.R. Eudaily, C.M. Jenness, D.G. MacWilkinson, Feasibility Study of the Transonic Biplane Concept for Transport Aircraft Application, NASA CR-132462, 1974

[18] M. M. Munk, The Minimum Induced Drag of Aerofoils, NACA R 121, 1921

[19] F.A. Khan, P. Krammer, D. Scholz, Preliminary Aerodynamic Investigation of Box-Wing Conf gurations Using Low Fidelity Codes, Deutscher Luft- und Raumfahrtkongress, Hamburg, 2010

[20] P. W. Jansen, R. E. Perez and J. R. R. A. Martins, Aerostructural Optimization of Nonplanar Lifting Surfaces, JOURNAL OF AIRCRAFT Vol. 47, No. 5, 2010

[21] M.A. Abramson, C. Audet, G. Couture, J.E. Dennis, Jr., and S. Le Digabel. The NOMAD project. Software available at http://www.gerad.ca/nomad.

[22] S. Le Digabel, Algorithm 909: NOMAD: Nonlinear optimization with the MADS algorithm. ACM Transactions on Mathematical Software, 37(4):44:1-44:15, 2011.

[23] A.Frediani, M. Gasperini, G. Saporito, A. Rimondi ,Development of a Prandtlplane Aircraft Conf guration, Available at http://www.prandtlplane.it, 2011.